Electronic structure, equation of state, and lattice dynamics of low-pressure Ge polymorphs

Brad D. Malone and Marvin L. Cohen
Department of Physics, University of California, Berkeley, California 94720, USA and Material Sciences Division, Lawrence Berkeley National Laboratory, Berkeley, California 94720, USA
(Received 17 April 2012; published 1 August 2012)

With the interest of obtaining more information on the low-energy phase diagram of germanium and its degree of similarity with silicon, we have performed first-principles calculations of the electronic structure and lattice dynamics of the R8, BC8, ST12, and hexagonal diamond structures of Ge. To aid future experimental investigation, we include predictions of the Raman-active frequencies of these phases as well as present the full phonon dispersion throughout the zone. Calculated equation of states within the local density approximation reveal a small pressure region where the R8 phase is energetically favored over the other metastable BC8 and ST12 structures, although the energy differences involved are relatively small and affected by the approximations used in the choice of pseudopotential.

DOI: 10.1103/PhysRevB.86.054101 PACS number(s): 64.30.Jk, 63.20.D−, 71.20.−b

I. INTRODUCTION

The phase diagrams of group IVa materials such as carbon, silicon, and germanium have generated substantial research interest not simply because of their status as prototypical insulators/semiconductors, but also because of their immense technological importance. The silicon and germanium phase diagrams have strong similarities in the structures reported both upon compression and decompression of experimental samples.[1] Both materials have the cubic diamond (cd) structure under ambient conditions and convert to the metallic β-Sn phase near a pressure of 10–12 GPa. Upon further compression both materials go through a similar sequence of high-pressure metallic phases, with the possible exception of the highest pressure transition being hexagonal close-packed (hcp) to face-centered cubic (fcc) in Si, while in Ge the highest pressure structure obtained thus far remains the hcp phase.[2]

If samples of Si or Ge are decompressed from the metallic β-Sn phase, they do not return to the cubic form at low temperatures, but instead go to a series of metastable phases. In Si, the slow decompression from the β-Sn phase results in the rhombohedral R8 phase at 9.4 GPa.[3] Further decompression results in the BC8 structure at 2 GPa.[4] In Ge, rapid release from the β-Sn structure to ambient pressure results in the BC8 structure, whereas slower release of pressure has resulted in the ST12 structure being recovered.[5] The ST12 phase has not yet been observed in Si and the R8 phase has not yet been definitively observed in Ge. The R8 phase of Ge has been reported in a single experiment but the result was not reproducible.[6] The phase transition pressures in Si are well determined experimentally and have been corroborated with theoretical calculations.[7,8] In Ge, on the other hand, fewer experimental and theoretical studies have been carried out. In particular, experimental studies of Ge often quench the pressure to ambient and then study the resulting phases with x-ray diffraction.[5,9] This is in contrast with experiments performed on Si in which the pressure has been reduced in small steps with the diffraction studies being performed at intermediate pressures in order to detect any resulting change in structure.[10]

From a theoretical standpoint, early calculations on the phase stability of Ge polymorphs report that the ST12 phase has a lower enthalpy than the BC8 phase over the pressure range 0–20 GPa.[11] At the time of these calculations the R8 phase of Si had yet to be discovered and was not considered in the study on Ge. Later, after the discovery of R8 Si,[10] density functional theory calculations predicted that the R8 phase of Ge was lower in enthalpy than that of the BC8 phase at moderate compression, and suggested that R8 might be obtained experimentally from compressing the BC8 phase.[12] The small differences in energy shown in the energy-volume relations for the three metastable phases made it difficult to estimate the transition pressure and thus no estimate was given.

The possibility of obtaining Ge in the R8 phase is an interesting one because R8 Si is believed to be a semiconductor[13,14] with interesting optical properties.[15,16] Additionally, the theoretical prediction of transition pressures between the metastable germanium phases would be of interest in helping to guide future experimental work in searching for metastable Ge structures, especially those which more carefully explored the pressure regime intermediate between ambient pressure and that where the β-Sn phase is stable. As noted earlier, the analogous theoretical transition pressures in Si are in good agreement with experimental observation,[7,8] and thus it might be expected for the same to be true in Ge.

In this work we focus on obtaining more information on the properties of Ge in the BC8, ST12, and R8 structures. In addition, we have performed calculations for the cubic, the hexagonal diamond, and β-Sn phases of Ge to have a complete description of the phases expected to be relevant below pressures of $\sim$10 GPa. We carry out detailed calculations on the structural properties, the electronic structure, the equations of state, and give estimates for the transition pressures between phases. Additionally, since except for the frequencies of the zone-center phonons for the BC8 and ST12 phases, little is known about the lattice dynamics of these phases.[17] Hence we compute the full phonon dispersions for the phases ST12, BC8, R8, and hexagonal diamond.

II. METHODS

Our calculations of the structural and electronic properties are done within the local density approximation (LDA) to

density functional theory (DFT). The plane-wave pseudopotential method[18,19] is used with a norm-conserving pseudopotential utilizing a nonlinear-core correction (NLCC)[20] to take into account the spatial overlap between the $3d$ electrons treated as core states and the $4s^2 4p^2$ electrons that were treated as valence. A kinetic energy cutoff of 40 Ry was found to result in highly accurate total energies and phonon frequencies. When structural relaxations were being performed, a higher cutoff of 70 Ry was used in order to have a highly converged stress tensor, which is known to converge more slowly with respect to the energy cutoff. This methodology is implemented in the QUANTUM ESPRESSO package.[21] Calculations of the phonon frequencies were also done within QUANTUM ESPRESSO using the density functional perturbation theory (DFPT) approach.[22] In this work we are very careful to ensure adequate sampling of the electronic and phonon Brillouin zones. Details of these samplings will be given later with the discussion of the corresponding results.

III. RESULTS

A. Structural descriptions

We have relaxed all structures with respect to all degrees of freedom to obtain the relaxed structures at zero pressure. Tests have been performed on the cubic phase of germanium to evaluate the quality of the pseudopotential in providing a good structural description. For cubic Ge a lattice constant of 5.58 Å was found, which underestimates the experimental lattice parameter of 5.66 Å by 1.4%.[23] The calculated bulk modulus is 77.2 GPa, which is in excellent agreement to the value of 75.8 GPa found experimentally.[24] Below we will provide the structural descriptions obtained and used in this work. More extensive descriptions of the space groups, bond length and angle distributions, etc. can be found in the references.

The ST12 structure of Ge can be described as a tetragonal unit cell with a 12 atom basis. The basis is fully specified with four internal parameters x, y, z, and α. We take as our starting point the structural parameters of Mujica and Needs which result from their theoretical relaxation as given in Ref. 11. Structural relaxation from these parameters changes little. We have used a $8 \times 8 \times 8$ grid to sample the Brillouin zone which ensures highly accurate forces and components of the stress tensor. Our final relaxed parameters for the tetragonal lattice are $a = 5.82$ Å with $c/a = 1.181$ Å. These compare well with the reported experimental values of 5.93 Å and 1.17707.[25] Our internal parameters of $x = 0.171$, $y = 0.370$, $z = 0.252$, and $\alpha = 0.0868$ compare well with the experimental parameters of $x = 0.1730$, $y = 0.3784$, $z = 0.2486$, and $\alpha = 0.0912$.[25] The bulk modulus of ST12 Ge is calculated to be 65.3 GPa, which is in excellent agreement with the value of 66 GPa calculated by Mujica and Needs.[11]

The BC8 structure of Ge is a body-centered cubic lattice with 8 atoms in the unit cell. It is completely specified by its lattice constant a and a single internal parameter x. We begin with the experimental lattice parameter as determined in Ref. 9, in which $a = 6.92$ Å, and take the internal parameter x to be that of the BC8 structure in Si, which experimentally is found to be 0.1033.[25] We then relax this starting structure with a mesh of size $12 \times 12 \times 12$ in the Brillouin zone. Our relaxed parameters are $a = 6.82$ Å and $x = 0.102$, in good agreement with both experiment and previous theory.[11] The calculated bulk modulus is determined to be 73.9 GPa, slightly smaller than the value for the cubic diamond phase and slightly higher than the value of 68 GPa calculated in Ref. 11.

As mentioned in the Introduction, no definitive experimental report has been made on the existence of the R8 phase in Ge and thus no experimental starting description is available. In this case we use the lattice constants known for Si in the R8 structure and scale them by the ratio of the Ge to the Si lattice constants parameters in the cubic phase. There are four internal parameters which specify the atomic positions in the R8 structure: u, x, y, and z. These values were given in Ref. 12 as a result of DFT calculations on the R8 structure in Ge and we take these values as our starting point (the lattice constants were not given in this work). As in the calculation of the BC8 structure, a mesh of $12 \times 12 \times 12$ was used for the integration over the Brillouin zone. Our relaxed lattice parameters for R8 Ge are $a_r = 5.91$ Å for the rhombohedral lattice vector with an angle of 109.95°. The obtained internal parameters for the R8 structure are $u = 0.285$, $x = 0.470$, $y = -0.027$, and $z = 0.277$. The values are similar, although slightly different, from those obtained in Ref. 12. Finally, the calculated bulk modulus of Ge in the R8 structure is 70.5 GPa.

Finally, in this work we also examine the hexagonal diamond structure of Ge. The initial parameters of the hexagonal lattice were taken to be $a = 3.96$ Å and $c = 6.57$ Å[26] with an internal parameter u taking the "ideal" value of 0.0625 (i.e., $1/16$). Our relaxed parameters of $a = 3.93$ Å, $c = 6.49$ Å, and $u = 0.0631$ are in excellent agreement with these values. The bulk modulus is obtained to be 78.2 GPa, in very close agreement to other LDA results in the literature.[27] The relaxation of this structure was performed with a mesh of $12 \times 12 \times 12$ in the Brillouin zone.

B. Electronic structure

The band structure of the ST12 Ge is shown in Fig. 1(a). Previous density functional calculations obtain a direct gap of size 0.7 eV about 70% of the way along the Γ-M line,[11] whereas those obtained via the empirical pseudopotential method (EPM) obtain a value of 1.47 eV.[28] Due to the well-known band gap problem inherent in DFT, the estimate provided by the EPM calculation is likely closer to the experimental value.[29] Our results are very similar to prior DFT results, although we find a direct gap of 0.56 eV just off the Γ-M line at (0.333,0.345,0). However, we also find that the fundamental gap is indirect. It is of magnitude 0.54 eV between the valence band maximum at (0.316,0.333,0.083) and the conduction band minimum at the location of the nonfundamental direct gap given above. This difference is simply attributed to the fact that we carried out a very fine sampling of the Brillouin zone ($60 \times 60 \times 60$) and therefore could resolve small deviations of the extremum positions off of the high-symmetry lines. Additionally, it should be noted that the valence band manifold in the vicinity of the valence band maximum has little dispersion and so the precise position of this gap could vary slightly depending on the details of the calculation.

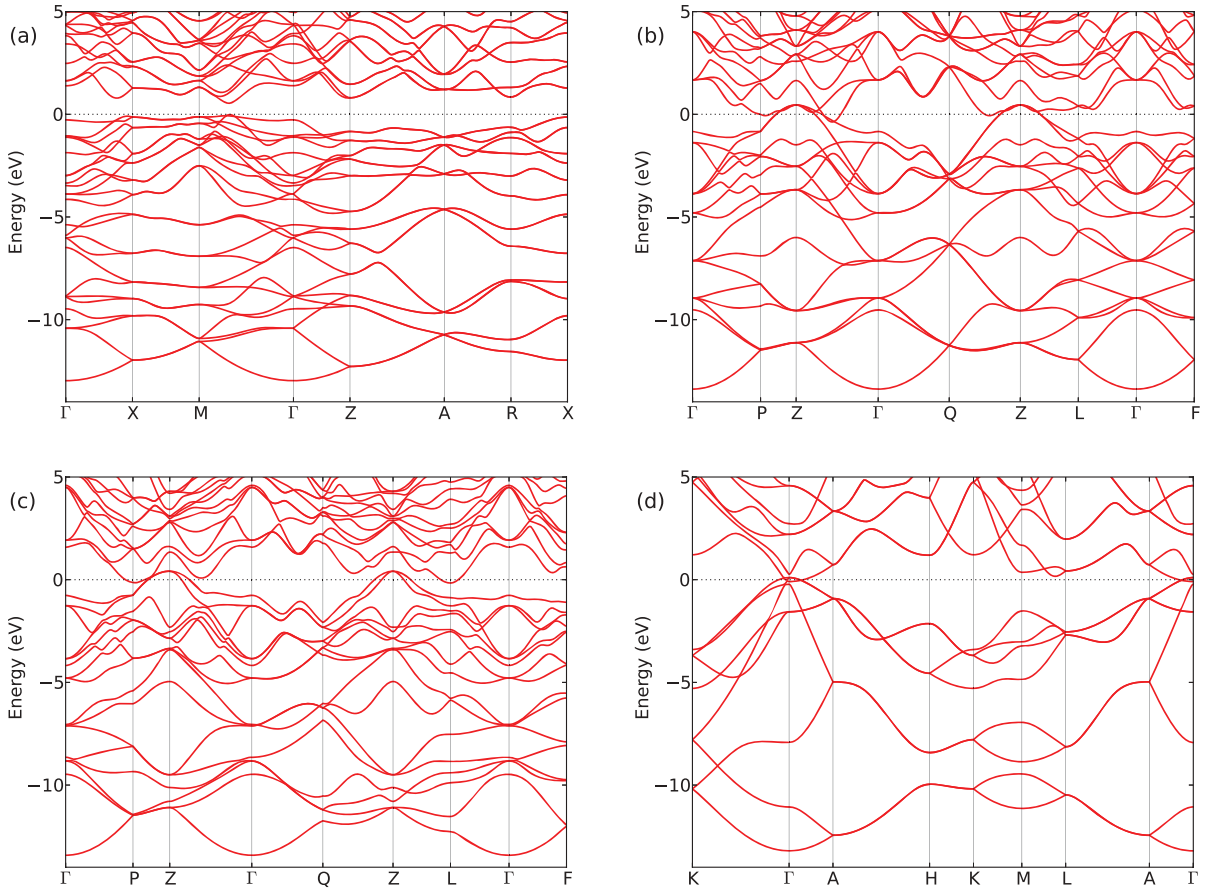

FIG. 1. (Color online) Band structures of Ge in the (a) ST12, (b) BC8, (c) R8, and (d) hexagonal diamond (lonsdaleite) phases. In (a) the zero of energy is set to zero at the valence band maximum (VBM), which lies just off the Γ-*M* line (see text). In (b), (c), and (d) the zero of energy is taken to be at the Fermi energy.

The BC8 phase of Ge, like that of Si,[7,14] is found to be semimetallic within DFT. The band structure of this phase is plotted in Fig. 1(b) throughout the high-symmetry points in the equivalent rhombohedral Brillouin zone. There is a direct overlap at the *Z* point (the *H* point in the body-centered cubic Brillouin zone). There is also a conduction-band-like state which drops below the Fermi level and has a minimum around 50% of the way along the Γ-*Z* line. This result is in good agreement with the results of Mujica and Needs.[11] The early results of Joannopoulos and Cohen with the EPM method find this conduction-band-like state to be higher in energy than that of the other conductionlike states at the *Z* point, which just touch the valence band maximum there and result in a zero-gap material.[28]

To our knowledge, the electronic structure of germanium in the R8 structure has not been explored previously. Using the close correspondence to silicon,[7] one would guess that R8 Ge would be semimetallic within DFT with an indirect overlap. Our calculations, shown in Fig. 1(c), confirm this expectation. The lowest conduction band occurs at the point *L*, and overlaps with the highest valence band at the point *Z*, by 0.57 eV. These are the same points where the band overlap occurs in the R8 phase of silicon. In the case of Si, both GW[14] and hybrid HSE[30] calculations predict that the band overlap present within DFT is lifted to obtain a small band gap semiconductor, and this prediction is consistent with recent experiments.[13] The examination of the electronic structure of R8 Ge at a level of theory beyond DFT is needed to evaluate this possibility, but lies outside the scope of the present work.

The hexagonal diamond phase is a phase which is believed to be typically recovered upon annealing depressurized samples of Si and Ge.[5] The band structure of this material is shown in Fig. 1(d) and we find a small overlap of 0.19 eV at Γ. This is similar to previous DFT theory suggesting a zero band gap at Γ[27] as well as EPM results which predict a direct gap of 0.55 eV at the zone center.[28] Again, because of the band gap underestimation within DFT, the EPM estimate is likely closer to what would be obtained experimentally.

C. Lattice dynamics

We have calculated the phonon dispersions for the ST12, BC8, R8, and hexagonal diamond phases of Ge throughout the entire Brillouin zone as shown in Fig. 2. The lattice parameters used in the calculations correspond to the zero-pressure theoretical relaxed structures. As a test, we have computed the zone-center optical phonon mode in the cubic phase of Ge and obtained a value of 298.2 cm^{-1}, which is in excellent agreement with the experimental result of 300.6 cm^{-1}.[31]

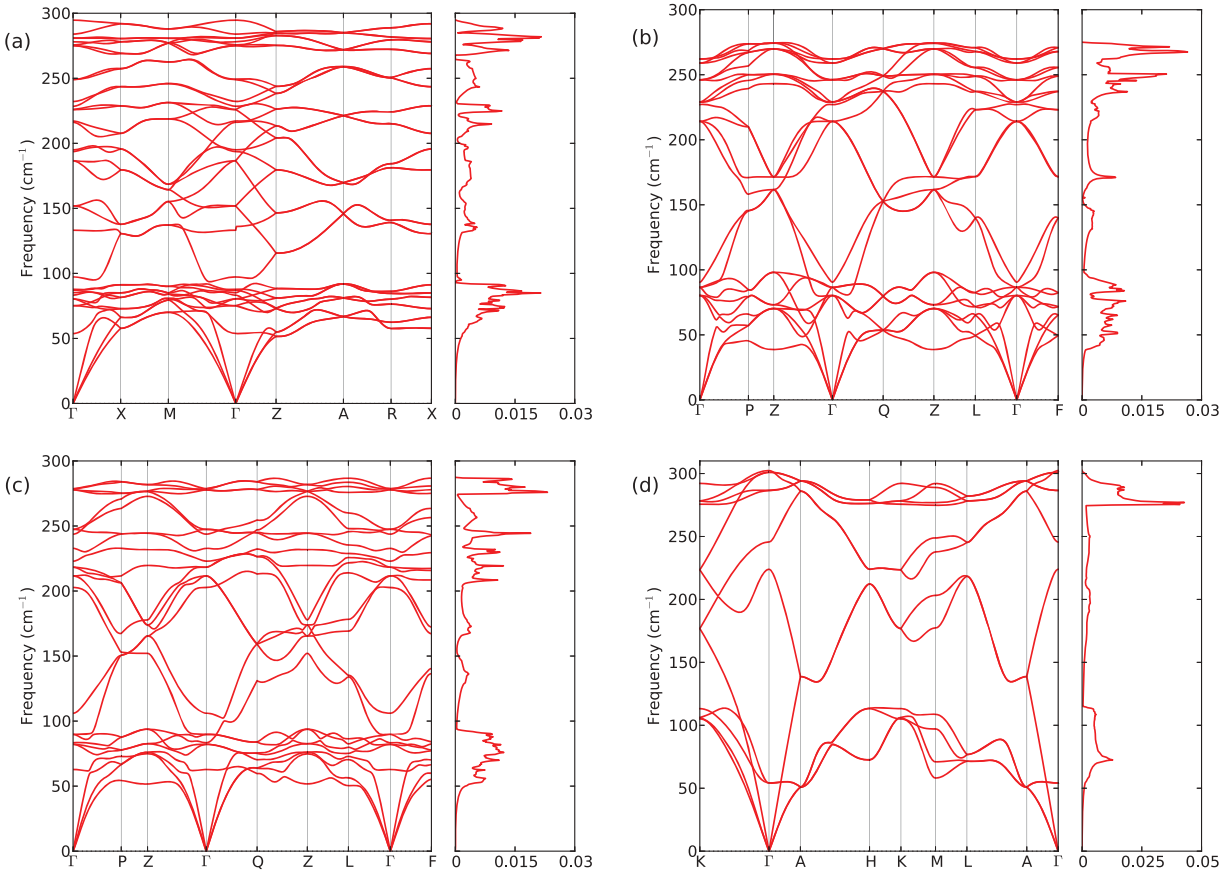

FIG. 2. (Color online) Phonon dispersions and phonon DOS for Ge in the (a) ST12, (b) BC8, (c) R8, and (d) hexagonal diamond (lonsdaleite) phases. In all plots the phonon DOS is normalized to 1.

The phonon dispersion of ST12 Ge is shown in Fig. 2(a). The full phonon dispersion was obtained by Fourier interpolation of a $4 \times 4 \times 4$ uniform grid of q points in the Brillouin zone. The electronic sampling in these calculations was on a shifted $5 \times 5 \times 5$ grid. The phonon dispersion of ST12 exhibits relatively flat bands in the region around 85 and 280 cm^{-1} leading to peaks in the phonon density of states (DOS) in those regions. An interesting feature is the presence of a slight discontinuity of approximately 3 cm^{-1} in the phonon frequency near Γ at ∼135 cm^{-1} as one goes from the $M \rightarrow \Gamma \rightarrow Z$ direction. The source of this discontinuity is the nonanalytic part of the force constant matrix which is present due to macroscopic polarization associated with this phonon mode. Typically one does not expect such contributions related to polar materials in a phase composed of only one element, but here it occurs due to the specific structure present in ST12. Phonon calculations we have performed on silicon in the ST12 structure show a similar discontinuity at this point. The calculated Raman active modes at Γ are (all frequencies in cm^{-1}): 54(B_1), 75(E), 80(E), 85(A_1), 87(B_1), 88(B_2), 97(A_1), 152(E), 187(E), 194(B_2), 195(A_1), 216(B_1), 217(B_2), 226(E), 232(B_1), 249(E), 275(E), 276(A_1), 281(E), 284(B_1), and 295(B_2).

The phonon dispersion for BC8 was obtained throughout the zone via Fourier interpolation from a uniform grid of $6 \times 6 \times 6$ phonon wave vectors in the Brillouin zone and a $10 \times 10 \times 10$ shifted grid for the sampling of the electronic states and is displayed in Fig. 2(b). The Raman-active modes in the BC8 structure are obtained as (all frequencies in cm^{-1}): 87(T_g), 214(T_g), 227(A_g), 246(T_g), and 259(E_g).

The phonon dispersion for the R8 phase of Ge is shown in Fig. 2(c). The electronic integration mesh, like in BC8, was performed on a $10 \times 10 \times 10$ shifted grid and a uniform grid of $6 \times 6 \times 6$ phonons were calculated to obtain the interpolated dispersion. Qualitatively, the phonon spectra for the R8 phase is similar to that found in the BC8 phase, although the differences present manifest themselves clearly in the calculated phonon DOS where the difference in the peak structure can be seen. The zone-center Raman active modes are found to be (all frequencies in cm^{-1}): 83(A_g), 90(E_g), 203(A_g), 212(E_g), 223(A_g), 244(A_g), 247(E_g), and 278(E_g).

Finally, the phonon dispersion of the hexagonal diamond (lonsdaleite) phase of Ge is shown in Fig. 2(d). These calculations were performed for a uniform grid of $6 \times 6 \times 6$ phonons with an electronic sampling on an $10 \times 10 \times 10$ shifted grid. The phonon DOS exhibits a prominent peak near a frequency of 275 cm^{-1}. The Raman-active modes for this phase are determined to be (all frequencies in cm^{-1}): 287(E_{2g}), 301(E_{1g}), and 302(A_{1g}).

D. Equation of state

In order to calculate coexistence pressures that may aid future experimental investigations, we have calculated the

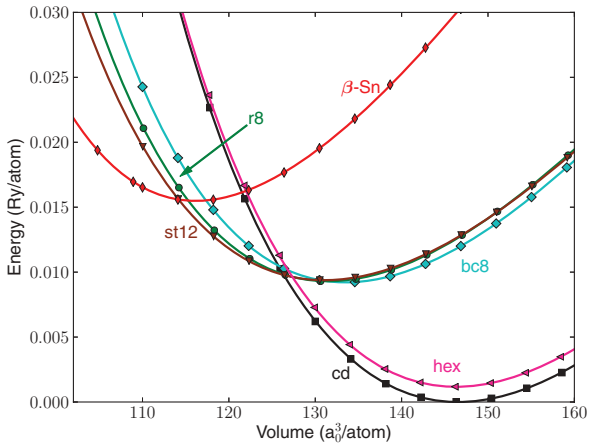

FIG. 3. (Color online) Energy-volume relations for low-pressure polymorphs of germanium. The markers correspond to the calculated data and the lines are fits to the Birch-Murnaghan equation of state. The equilibrium energy of the cubic phase is located at zero energy.

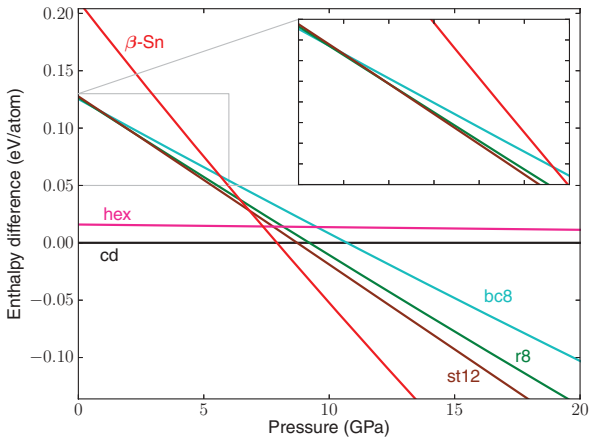

FIG. 5. (Color online) Enthalpy as a function of pressure for low-pressure polymorphs of germanium. All enthalpies are taken relative to that of the cubic phase, which is shown at zero. The inset is a zoomed-in view showing the BC8-R8-ST12 transition region.

energy-volume relations for the cubic, BC8, R8, ST12, hexagonal diamond, and β-Sn structures of Ge. These calculations are performed by calculating the total energies of each structure while fully relaxing the cell and ion positions at fixed volume. The resulting $E(V)$ curve is fit with a Birch-Murnaghan equation of state.[32] The results are shown in Fig. 3. Pressure-volume curves are shown in Fig. 4 and are obtained via numerical differentiation of the $E(V)$ relations. Knowledge of $E(V)$ and $V(P)$ allows for the determination of the enthalpy as a function of pressure, $H(P) = E[V(P)] + PV(P)$, which is shown in Fig. 5. It is simpler to obtain coexistence pressures from the enthalpy-pressure curves than from the equivalent "common tangent" approach to the energy-volume relations.

From the results of Fig. 5, we can calculate transition pressures between the various phases. The first of these we will examine is that of the cubic $\rightarrow$ β-Sn transition that occurs experimentally at 10.5 GPa.[33] We find this transition at a pressure of 7.9 GPa, which underestimates the transition in comparison to the experimental value. This result is in

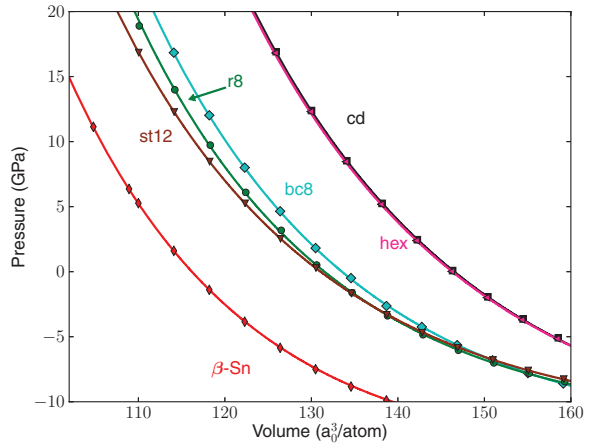

FIG. 4. (Color online) Pressure-volume relations for low-pressure polymorphs of germanium. The markers correspond to the calculated data and the lines are taken from numerical differentiation from the $E(V)$ curves shown in Fig. 3.

reasonable agreement with that obtained in previous theoretical calculations by Mujica *et al.* within the LDA, who also underestimate the experimental transition pressure, predicting the transition at 6 GPa.[11] The early LDA results of Yin and Cohen[34] also underestimate the transition pressure at a value of 9.6 GPa, although in this work the coexistence pressure is higher and closer to the experimental value partly because of the use of the Wigner formula[35] for the exchange-correlation energy.[36] The underestimation of the cubic $\rightarrow$ β-Sn transition pressure within LDA functionals occurs in both Si and Ge and is improved upon in the inclusion of gradient corrections to the exchange correlation functional which increase the transition pressure and bring it closer to the experimental value.[36,37] This behavior was explained as being the result of a greater lowering of the total energy for systems with more inhomogeneous charge densities upon going from the LDA to the generalized gradient approximation (GGA).[36] Since the cubic diamond phase has a more inhomogeneous charge density than that of the metallic β-Sn phase, its total energy is lowered by a greater amount upon going to the GGA. This results in a larger difference in energies at equilibrium between the two phases and thus a larger transition pressure.[36]

An interesting observation, originally seen in the results of Mujica *et al.*,[11] is that if the cubic $\rightarrow$ β-Sn transition pressure were corrected to the experimental value of 10.5 GPa, that this would result in a region of stability for the ST12 phase because the enthalpy for the cubic diamond phase becomes equal to that of ST12 at 8.7 GPa. This is just under 2 GPa from the experimental cubic-β-Sn coexistence pressure. Although there have been reports recently in nanocrystalline samples of Ge that the ST12 phase appears to be more stable than previous experiments have suggested,[38] we are not aware of any experimental results that have reported this possible region of stability at higher pressures.

With regards to the phases obtained upon decompression from β-Sn, namely the R8, BC8, and ST12 phases of Ge, we obtain regions of metastability (compared to the cubic phase) for all three phases. This can be seen from the inset of Fig. 5. The ST12 phase of Ge is found to transition to the

R8 structure at 2.0 GPa, which remains the lowest enthalpy of these three phases until 0.65 GPa when it transitions to the BC8 phase.

Predictions of phase stability are known to be sensitive, in some cases strongly so, to the underlying treatment of exchange and correlation effects. This was discussed above in relation to the cubic $\rightarrow$ β-Sn transition. The small enthalpy differences between the BC8, R8, and ST12 phases near the predicted transitions as seen in Fig. 5 suggest that these transitions might also be sensitive to the functional used. In order to illustrate this, we have repeated the equation of state calculations with another pseudopotential which includes both the semicore 3*d* states explicitly and in addition treats the correlation-exchange energy in the PW91 GGA functional of Perdew and Wang.[39,40] The purpose of this is not to systematically evaluate the effects of gradient corrections, the inclusion of semicore states, etc., but to simply obtain the results that would be expected if different choices were made in the pseudopotential construction. As expected with the GGA, the lattice constant of cubic germanium is overestimated, in this case by 1.7%, in comparison to experiment. The bulk modulus obtained is 60.2 GPa, which compares less favorably to the experimental value of 75 GPa that we obtained with our calculations within the LDA. This underestimation of the bulk modulus in Ge within GGA is consistent with results elsewhere in the literature.[27,36] With the GGA functional, the transition pressure of the cubic $\rightarrow$ β-Sn transition is pushed up to 10 GPa, in close agreement with the experimental value of 10.5 GPa, as expected due to the effect of the GGA on systems with large differences in their degree of charge homogeneity. In the GGA calculations the pressure region where R8 is favored over BC8 or ST12 is no longer present, and BC8 is found to have a coexistence pressure with ST12 at 3.6 GPa. The enthalpies of the ST12 and β-Sn phases become equal at a pressure of 8.4 GPa, which differs from the 6.8 GPa we find in the calculation within the LDA.

Changing the exchange-correlation functional and altering the split between core and valence electrons changes the prediction of a metastable R8 phase in Ge means that we cannot draw firm conclusions that this is the case. This is not surprising because of the closeness in enthalpy of the three enthalpy curves in both of our calculations. However, it must be pointed out that GGA calculations do not uniformly improve the results in relation to the LDA.[41] The strong effect of simply including gradient corrections on the cubic-β-Sn transition due to the differences in charge homogeneity is not expected to exist in relation to the transitions between BC8, R8, and ST12, which all have similar bonding characteristics. Furthermore, the calculations performed with the LDA result in a much more accurate bulk modulus than that in the GGA, which has a direct and obvious relationship to the $E(V)$ relations and thus the calculated transition pressures. Finally, it is well-known that DFT has shortcomings in its treatment of localized states. In germanium this results in binding energies which are too shallow in relation to experiment by about 5 eV for the semicore 3*d* states,[42] and thus their inclusion into the valence might also induce some errors in the computed quantities.

IV. CONCLUSION

In this work we have calculated the electronic structure, phonon dispersions, and the phase diagram of the low pressure phases of germanium, namely those of hexagonal diamond, ST12, R8, and BC8. Our electronic structures are in good agreement with previous calculations and suggest BC8 and R8 to be semimetallic, at least within DFT, while ST12 is semiconducting. Calculations of the lattice dynamics of these phases have been performed and Raman-active phonon frequencies have been identified which may help aid future experimental work in the identification of metastable germanium phases in diamond anvil cell and nanoindentation experiments.

Calculations of the equation of state of these phases find regions of metastability of the BC8, R8, and ST12 phases of germanium, which suggests that the R8 phase of Ge might be obtained from compression of the BC8 phase or a partial reduction of pressure upon obtaining ST12. However, because of the small energy differences involved, this result is sensitive to choices made in constructing the pseudopotential, and thus firm predictions on the metastability of the R8 structure in Ge are difficult to make at this time. Further experimental studies could help shed light on this matter, and the Raman-active phonon modes calculated here will hopefully be of use in helping to identify these phases.

ACKNOWLEDGMENTS

We thank Bianca Haberl, Jodie Bradby, and Jim Williams for helpful and ongoing discussion and suggestions. This work was supported by National Science Foundation Grant No. DMR10-1006184 and by the Director, Office of Science, Office of Basic Energy Sciences, Materials Science and Engineering Division, US Department of Energy under Contract No. DE-AC02-05CH11231. Computational resources have been provided by DOE at Lawrence Berkeley National Laboratory's NERSC facility.

[1] A. Mujica, A. Rubio, A. Muñoz, and R. J. Needs, Rev. Mod. Phys. **75**, 863 (2003).
[2] F. J. Ribeiro and M. L. Cohen, Phys. Rev. B **62**, 11388 (2000).
[3] R. J. Nelmes and M. I. McMahon, Semicond. Semimetals **54**, 145 (1998).
[4] R. O. Piltz, J. R. Maclean, S. J. Clark, G. J. Ackland, P. D. Hatton, and J. Crain, Phys. Rev. B **52**, 4072 (1995).
[5] R. J. Nelmes, M. I. McMahon, N. G. Wright, D. R. Allan, and J. S. Loveday, Phys. Rev. B **48**, 9883 (1993).
[6] A. G. Lyapin, V. V. Brazhkin, S. V. Popova, and A. V. Sapelkin, Phys. Status Solidi B **198**, 481 (1996).
[7] B. G. Pfrommer, M. Côté, S. G. Louie, and M. L. Cohen, Phys. Rev. B **56**, 6662 (1997).
[8] B. D. Malone and M. L. Cohen, Phys. Rev. B **85**, 024116 (2012).

[9]C. H. Bates, F. Dachille, and R. Roy, Science **147**, 860 (1965).
[10]J. Crain, G. J. Ackland, J. R. Maclean, R. O. Piltz, P. D. Hatton, and G. S. Pawley, Phys. Rev. B **50**, 13043 (1994).
[11]A. Mujica and R. J. Needs, Phys. Rev. B **48**, 17010 (1993).
[12]A. Mujica, S. Radescu, A. Muñoz, and R. J. Needs, Phys. Status Solidi B **223**, 379 (2001).
[13]S. Ruffell, K. Sears, A. P. Knights, J. E. Bradby, and J. S. Williams, Phys. Rev. B **83**, 075316 (2011).
[14]B. D. Malone, J. D. Sau, and M. L. Cohen, Phys. Rev. B **78**, 035210 (2008).
[15]B. D. Malone, J. D. Sau, and M. L. Cohen, Phys. Rev. B **78**, 161202 (2008).
[16]M. L. Cohen and B. D. Malone, J. Appl. Phys. **109**, 102402 (2011).
[17]F. Coppari, J. C. Chervin, A. Congeduti, M. Lazzeri, A. Polian, E. Principi, and A. Di Cicco, Phys. Rev. B **80**, 115213 (2009).
[18]J. Ihm, A. Zunger, and M. L. Cohen, J. Phys. C **12**, 4409 (1979).
[19]M. L. Cohen, Phys. Scr. **T1**, 5 (1982).
[20]S. G. Louie, S. Froyen, and M. L. Cohen, Phys. Rev. B **26**, 1738 (1982).
[21]P. Giannozzi, S. Baroni, N. Bonini, M. Calandra, R. Car, C. Cavazzoni, D. Ceresoli, G. L. Chiarotti, M. Cococcioni, I. Dabo *et al.*, J. Phys.: Condens. Matter **21**, 395502 (2009).
[22]S. Baroni, S. de Gironcoli, A. Dal Corso, and P. Giannozzi, Rev. Mod. Phys. **73**, 515 (2001).
[23]J. Donohue, in *The Structure of the Elements* (John Wiley, New York, 1974).
[24]L. J. Bruner and R. W. Keyes, Phys. Rev. Lett. **7**, 55 (1961).
[25]J. S. Kasper and S. M. Richards, Acta Crystallogr. **17**, 752 (1964).
[26]S.-Q. Xiao and P. Pirouz, J. Mater. Res. **7**, 1406 (1992).
[27]S. Q. Wang and H. Q. Ye, J. Phys.: Condens. Matter **15**, L197 (2003).
[28]J. D. Joannopoulos and M. L. Cohen, Phys. Rev. B **7**, 2644 (1973).
[29]As a point of reference, our calculations find the band gap of cubic germanium to be 0.24 eV at Γ for the LDA-relaxed structure.
[30]B. D. Malone and M. L. Cohen, J. Phys.: Condens. Matter **24**, 055505 (2012).
[31]D. Olego and M. Cardona, Phys. Rev. B **25**, 1151 (1982).
[32]F. Birch, Phys. Rev. **71**, 809 (1947).
[33]A. Werner, J. A. Sanjurjo, and M. Cardona, Solid State Commun. **44**, 155 (1982).
[34]M. T. Yin and M. L. Cohen, Solid State Commun. **38**, 625 (1980).
[35]E. Wigner, Phys. Rev. **46**, 1002 (1934).
[36]N. Moll, M. Bockstedte, M. Fuchs, E. Pehlke, and M. Scheffler, Phys. Rev. B **52**, 2550 (1995).
[37]R. G. Hennig, A. Wadehra, K. P. Driver, W. D. Parker, C. J. Umrigar, and J. W. Wilkins, Phys. Rev. B **82**, 014101 (2010).
[38]S. J. Kim, O. K. Quy, L.-S. Chang, E. A. Stach, C. A. Handwerker, and A. Wei, J. Mater. Chem. **20**, 331 (2010).
[39]J. P. Perdew, J. A. Chevary, S. H. Vosko, K. A. Jackson, M. R. Pederson, D. J. Singh, and C. Fiolhais, Phys. Rev. B **46**, 6671 (1992).
[40]Specifically, we use the pseudopotential Ge.pw91-n-van.UPF provided in the QUANTUM ESPRESSO pseudopotential library.
[41]A. García, C. Elsässer, J. Zhu, S. G. Louie, and M. L. Cohen, Phys. Rev. B **46**, 9829 (1992).
[42]M. Rohlfing, P. Krüger, and J. Pollmann, Phys. Rev. B **56**, 7065 (1997).